Electron-atom scattering resonances: Complex-scaled multiconfigurational spin-tensor electron propagator method for B^-shape resonances

Tsogbayar Tsednee and Danny L. Yeager[*]
Department of Chemistry, Texas A&M University, College Station, Texas 77843, USA
(Received 24 April 2015; published 9 June 2015)

We develop the complex-scaled multiconfigurational spin-tensor electron propagator (CMCSTEP) technique for the theoretical determination of resonance parameters with electron-atom–molecule systems including open-shell and highly correlated (nondynamical correlation) atoms and molecules. The multiconfigurational spin-tensor electron propagator method developed and implemented by Yeager and his coworkers in real space gives very accurate and reliable ionization potentials and electron affinities. The CMCSTEP method uses a complex-scaled multiconfigurational self-consistent field state as an initial state along with a dilated Hamiltonian where all of the electronic coordinates are scaled by a complex factor. We apply the CMCSTEP and the related M_1 methods to get the B^- shape resonance parameters using $14s11p$ and $14s11p5d$ basis sets with $1s2s2p3s$, $1s2s2p3s3p$, $1s2s2p3d$, $2s2p3s3p$, $2s2p3d$, and $2s2p3s3p3d$ complete active spaces. The CMCSTEP and M_1 resonance positions and widths are obtained for the $1s^22s^22p^2\,{}^1D$, $1s^22s2p^3\,{}^3D$, and $1s2s^22p^3\,{}^3D$, ${}^3S$, and ${}^3P$ shape resonances.

DOI: 10.1103/PhysRevA.91.063405 PACS number(s): 33.35.+r, 31.15.−p, 32.10.Hq

I. INTRODUCTION

Resonances in electron-atom or electron-molecule scattering processes have attracted much attention. They play major roles in electron transport and energy exchange between electronic and nuclear motions, in vibrational excitation of molecules or molecular ions by electron impact, in dissociative attachments and recombination [1,2], and as a mechanism for DNA damage by low-energy electrons [3,4].

In order to avoid direct calculation of an outgoing wave in resonance problems, we use a complex coordinate scaling (CS) technique, which was first proposed by Combes and co-workers [5,6] and Simon [7] in the early 1970s. In this approach the electronic coordinates r of the Hamiltonian are scaled (or dilated) by a complex parameter η as $r \to \eta r$, where $\eta = \alpha e^{i\theta}$ with $\alpha > 0$ and $\theta \in (-\pi,\pi)$. Under this transformation, the bound states are real and are unchanged by complex scaling and the continua of the complex-scaled Hamiltonian $\bar{H}$ is rotated by an angle 2θ at each threshold such that the continuum states appear as complex eigenvalues of the complex-scaled Hamiltonian $\bar{H}$. The resonance parameters $E = E_r - i\frac{\Gamma_r}{2}$ hidden in the continua are exposed in complex space for some suitable η, where E_r and Γ_r are the resonance position and width of that resonance state, respectively.

Other alternative methods have included the complex absorbing potential (CAP) [8–11] instead of CS. Both CS and CAP methods can be developed and programmed from bound-state electronic structure codes. Complex absorbing potential methods have not been shown conclusively to be superior to standard complex scaling.

Previously, we developed and used the quadratically convergent Δ (total energy difference) complex-scaled multiconfigurational self-consistent field [12,13] (CMCSCF) method with step length control to obtain the resonance parameters. In real space, the multiconfigurational self-consistent field (MCSCF) method with a small complete active space (CAS) has been shown to be a very effective method to describe nondynamical and some dynamical correlation correctly and is computationally cheaper than very large or full configuration-interaction calculations [14] while still incorporating the fundamental physics of what is going on.

Based on the CMCSCF initial state, we also developed a method termed the M_1 method [13,15], in which the complex M_1 matrix is constructed from the first block of the M matrix defined in the multiconfigurational spin-tensor electron propagator (MCSTEP) method [16–20]. This block allows for only simple electron removal and addition to multiconfigurational based orbitals with no more complicated processes allowed to mix in.

The MCSTEP method, however, includes many additional operators that allow for more complicated electron ionization and attachment processes to be included. The MCSTEP method is designed to calculate reliably the ionization potentials (IPs) [18–20] and electron affinities (EAs) [21,22] for atoms and molecules that cannot generally be handled accurately and efficiently by perturbation or other methods. In addition to simple electron addition operators to all orbitals as in the M_1 method, the MCSTEP method includes operators that allow for electron removal and electron addition to all orbitals to excited states within the CAS [16–20]. With the MCSTEP method both initial and final states have pure space and spin symmetry even for open-shell initial and final states. In complex space, the M_1 and complex-scaled MCSTEP (CMCSTEP) methods use CMCSCF states as reference or initial states along with $\bar{H}$.

Both the CMCSCF and M_1 methods have been previously used efficiently to study the ${}^2P$ Be^- shape resonance [12,13,15]. The CMCSTEP method was first employed to study the ${}^2P$ Be^- shape resonance problem [23]. The Be atom is the prototypical system with nondynamical correlation since the ground initial state is about 10% $1s^22p^2$.

The existence of the B^- ion was first reported on by Branscomb and Smith in 1956 [24]. The first quantitative measurement of B^- was the EA determination by Feigerle *et al.* [25] using the laser-photodetached electron spectroscopy.

[*]yeager@mail.chem.tamu.edu

They showed that the B^- ion was stably formed in the $2p^2\,{}^3P$ state. Further experimental work had been carried out by Liu *et al.* [26], Lee *et al.* [27,28], Kristensen *et al.* [29], Scheer *et al.* [30], and Berrah *et al.* [31].

Theoretical work for the B^- ion first focused on calculating the EA and is summarized in Ref. [32]. Accurate calculations for the EA for B^- were carried out by Sundholm and Olsen [33] and Froese Fischer *et al.* [34], both using the large multiconfiguration Hartree-Fock methods.

In this work we implement the M_1 and CMCSTEP methods for the B^- shape resonance problems using $14s11p$ and $14s11p5d$ basis sets with several CASs and compare our results with previous results. Previous application of the CMCSTEP method was to a closed-shell atomic system, the ${}^2P$ Be^- shape resonance [23], however, the present work applies to an open-shell atomic system, such as the B^- shape resonances. The reason we implement this method for the resonance problem is that the MCSTEP method in real space works exceptionally well and gives accurate and reliable values of vertical IPs and EAs for general atomic and molecular systems that are consistent with experimental measurements [21,22,35–38]. Hence, we expect that the CMCSTEP method will give reliable values of resonance parameters.

The paper is organized as follows. In Sec. II we discuss the theory of the CMCSTEP method. In Sec. III we present and discuss our results and the experimental and theoretical results of others. A summary and conclusions follow in Sec. IV.

II. THEORY

The complex-scaled electronic Hamiltonian $\bar{H}$ is non-Hermitian. It is complex symmetric. This causes the wave function $|\psi_m\rangle$ to be complex conjugate biorthogonal where $\langle\psi_i^*|\psi_j\rangle = \delta_{ij}$ (the asterisk denotes the complex conjugate) [39]. It is shown that creation operators are introduced as $a^T = a^\dagger = (a^*)^\dagger$ rather than $a^\dagger$, with the usual anticommutation relations for creation and annihilation operators still hold by changing the dagger into T [40,41].

Therefore, the CMCSTEP may be formulated in the same way as the MCSTEP via single-particle Green's-function or electron propagator methods [16–20] or the superoperator formalism [42] with the modified second quantization operators and $\bar{H}$. We will not discuss the MCSTEP details here, since they can be found in Refs. [16–20].

Complex-scaled MCSTEP IPs and attachment energies (AEs) are obtained from the following the complex generalized eigenvalue problem:

$$\mathbf{MX}_f = \omega_f \mathbf{NX}_f, \tag{1}$$

where

$$M_{rp} = \sum_{\Gamma}(-1)^{S_0-\Gamma-S_f-\gamma_r} W(\gamma_r\gamma_p S_0 S_0;\Gamma S_f) \times(2\Gamma+1)^{1/2}\langle NS_0||\{h_r^*(\bar{\gamma}_r),\bar{H},h_p(\gamma_p)\}||NS_0\rangle, \tag{2}$$

$$N_{rp} = \sum_{\Gamma}(-1)^{S_0-\Gamma-S_f-\gamma_r} W(\gamma_r\gamma_p S_0 S_0;\Gamma S_f) \times(2\Gamma+1)^{1/2}\langle NS_0||\{h_r^*(\bar{\gamma}_r),h_p(\gamma_p)\}||NS_0\rangle, \tag{3}$$

Here ω_f is the IP or AE from the N-electron initial tensor state $|NS_0\rangle$ with spin S_0 to the $N\pm 1$ electron final ion tensor state $|N\pm 1S_f\rangle$, which has spin S_f, W is the usual Racah coefficient, $h_p(\gamma_p)$ and $h_p^*(\bar{\gamma}_r)$ are tensor operator versions of members of the operator manifold with ranks γ_p and γ_r, respectively, $\{\,,\}$ is the anticommutator

$$\{A,B\} = AB + BA, \tag{4}$$

and $\{\,,\,,\}$ is the symmetric double anticommutator

$$\{A,B,C\} = \tfrac{1}{2}(\{A,[B,C]+\{[A,B],C\}\}). \tag{5}$$

The CMCSTEP method uses a CMCSCF initial state with a fairly small CAS and couples tensor ionization and attachment operators to a tensor initial state to a final state that has the correct spin and spatial symmetry even if the initial state is open shell and/or highly correlated.

Following [23], we can report on the resonance parameter $\epsilon_{\rm CMCSTEP}$ obtained from the CMCSTEP method:

$$\epsilon_{\rm CMCSTEP}(\eta) = \omega_f^{\rm CMCSTEP} + E_c^N - E_0^N, \tag{6}$$

where $\omega_f^{\rm CMCSTEP} \equiv \omega_f$ is calculated from Eq. (1). In the case of M_1 calculations it is obtained from the M_1 complex eigenvalue problem [13] and we reported on results based on complex eigenvalues $\omega_f^{M_1}$ rather than the $\omega_f^{\rm CMCSTEP}$ in Eq. (6). Here E_c^N is the CMCSCF energy at the stabilized point and E_0^N is the MCSCF (real) energy for the $1s^2 2s^2 2p\,{}^2P$ ground state.

The optimal values of α and θ enable one to estimate the resonance parameters and can be found by the system of equations

$$\frac{\partial E}{\partial\alpha} = \frac{\eta}{\alpha}\frac{\partial E}{\partial\eta} = 0, \tag{7}$$

$$\frac{\partial E}{\partial\theta} = -i\eta\frac{\partial E}{\partial\eta} = 0, \tag{8}$$

which forms the trajectory method by determining $E(\alpha_{\rm opt},\theta_{\rm opt})$ corresponding to the stability (loops, kinks, inflections, or any kind of slowdown) in the plots of Im(E) as a function of Re(E) evaluated as a series of α values (α trajectory) and a series of θ values (θ trajectory) [43,44].

TABLE I. Summary of theoretical calculations for the B^- $1s^2 2s^2 2p^2\,{}^1D$ shape resonance relative to the B $1s^2 2s^2 2p\,{}^2P$ ground state.

Method	Basis set CAS	α	$\theta_{\rm opt}$ (rad)	E_r (eV)	Γ_r (eV)
M_1	$14s11p$-$2s2p3s3p$	1	0.22	0.161	0.0486
M_1	$14s11p$-$1s2s2p3s$	1	0.21	0.180	0.0575
M_1	$14s11p5d$-$2s2p3d$	1	0.25	0.156	0.0538
M_1	$14s11p5d$-$2s2p3s3p3d$	1	0.21	0.143	0.0574
CMCSTEP	$14s11p$-$2s2p3s3p$	1	0.16	0.185	0.0441
CMCSTEP	$14s11p$-$1s2s2p3s$	1	0.21	0.180	0.0575
CMCSTEP	$14s11p5d$-$2s2p3d$	1	0.25	0.158	0.0536
CMCSTEP	$14s11p5d$-$2s2p3s3p3d$	1	0.28	0.126	0.0613

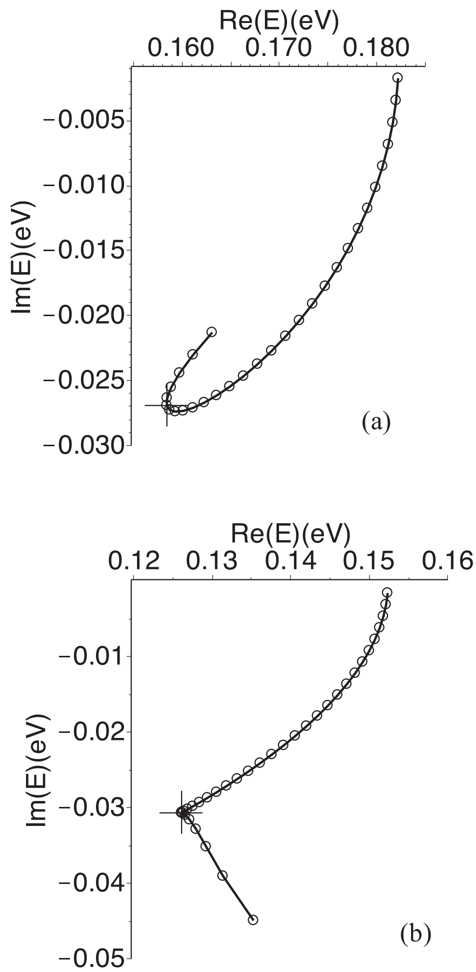

FIG. 1. The θ trajectories for B^- $1s^22s^22p^2\ ^1D$ shape resonances obtained from the CMCSTEP method. The curves correspond to the (a) basis set $14s11p5d$-$2s2p3d$ CAS and (b) $14s11p5d$-$2s2p3s3p3d$ CAS and the cross shows a stabilized point. The computational parameters are $\alpha = 1$ and $\Delta\theta = 0.01$ rad.

III. RESULTS AND DISCUSSION

In this study we investigate the shape resonance problems for the lowest and first excited states of the B^- ion using the M_1 and CMCSTEP methods. The B atom is an open-shell system and has a ^2P ground state. The principal configuration of the ground state is $1s^22s^22p$. Thus it requires the full power of a tensor formalism of the CMCSTEP approximation, in which spin symmetry is always correctly handled [16–20]. Recently, we presented the M_1 and CMCSTEP calculations for the low-lying ^2P Be^- shape resonance problem, where the ground state is ^1S, i.e., totally symmetric in spin and space [23].

TABLE II. Summary of theoretical calculations and experimental measurement for the B^- $1s^22s^22p^2\ ^1D$ shape resonance relative to the B $1s^22s^22p\ ^2P$ ground state.

Reference	E_r (eV)	Γ_r (eV)
[46]	−0.61	
[47]	0.375	
[48]	0.45	0.11
[49]	0.006	
[50]	0.275	
[51]	0.095	0.054
this work		
M_1	0.143	0.0574
CMCSTEP	0.126	0.0613
Expt. [28]	0.104 ± 0.008	0.068 ± 0.025

TABLE III. Same as in Table I, but for the B^- $1s^22s2p^3\ ^3D$ shape resonance.

Method	Basis set CAS	α	θ_{opt} (rad)	E_r (eV)	Γ_r (eV)
M_1	$14s11p$-$1s2s2p3s$	1	0.38	4.22	1.13
M_1	$14s11p$-$1s2s2p3s3p$	1	0.41	4.13	1.23
M_1	$14s11p5d$-$1s2s2p3d$	1	0.38	4.11	1.09
CMCSTEP	$14s11p$-$1s2s2p3s$	1	0.35	4.49	1.44
CMCSTEP	$14s11p$-$1s2s2p3s3p$	1	0.39	4.41	1.60
CMCSTEP	$14s11p5d$-$1s2s2p3d$	1	0.36	4.38	1.43

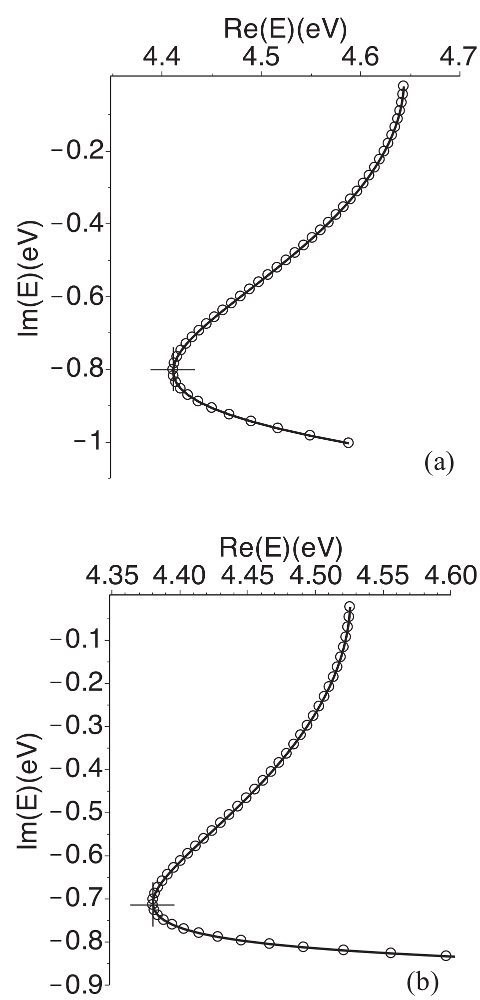

FIG. 2. The θ trajectories for (c) B^- $1s^22s2p^3\ ^3D$ shape resonances obtained from the CMCSTEP method. The curves shown correspond to the (a) basis set $14s11p$-$1s2s2p3s2p$ CAS and (b) $14s11p5d$-$1s2s2p3d$ CAS and the cross shows a stabilized point. Computational parameters are $\alpha = 1$ and $\Delta\theta = 0.01$ rad.

TABLE IV. Same as in Table II, but for the B^- $1s^22s2p^3\ {}^3D$ shape resonance.

Reference	E_r (eV)	Γ_r (eV)
[52]	4.22	1.09
[57]	4.35 ± 0.07	0.82
this work		
M_1	4.11	1.09
CMCSTEP	4.38	1.43
Expt. fit [29]	4.31	1.16

For these resonance problems, we use initially the $14s11p$ uncontracted basis set, which is based on the s and p functions in the cc-pVTZ basis set [45] and then we added d functions to it using a geometric progression with a view to account for the diffuse nature of the resonances. Since for an accurate IP of B, a larger $2s2p3s3p3d$ CAS that enables more correlation is reliable [20], we employ basis sets $14s11p$ and $14s11p5d$ with $2s2p3s3p$, $2s2p3d$, $2s2p3s3p3d$, $1s2s2p3s$, $1s2s2p3s3p$, and $1s2s2p3d$ CASs as appropriate basis sets in this calculation. The first three CASs have three electrons and last three CASs have five electrons in them for the CMCSCF initial state. Most typical basis sets are designed for total energies of low-lying states where tighter functions are necessary rather than for resonance calculations where what is needed are basis functions to describe near the continuum as well.

A. The $1s^22s^22p^2\ {}^1D$ shape resonance

We compute the B^- $1s^22s^22p^2\ {}^1D$ shape resonance parameters using the M_1 and CMCSTEP methods. We use the CMCSCF lowest ${}^2P$ state as the neutral initial state in this CMCSTEP calculation.

In Table I we show a summary of our obtained values with the M_1 and CMCSTEP methods for the B^- $1s^22s^22p^2\ {}^1D$ shape resonance for $14s11p$ and $14s11p5d$ basis sets with different CASs. In rows 2–5 and 6–9 of Table I we show results from the M_1 and CMCSTEP calculations, respectively. Widths shown in Table I are small and consistent with each other, while the values of the positions show a convergence with an increase of basis sets with relatively large CASs. In these calculations we use the initial CMCSCF state and MCSCF ground ${}^2P$ state energies for E_c^N and E_0^N [see Eq. (6)], respectively, to obtain resonance parameters for the B^- $1s^22s^22p^2\ {}^1D$ shape resonance with respect to the B $1s^22s^22p\ {}^2P$ ground state.

In Fig. 1 we show the θ trajectories for the B^- $1s^22s^22p^2\ {}^1D$ shape resonance obtained from the CMCSTEP method with the basis set $14s11p5d$-$2s2p3d$ CAS [Fig. 1(a)] and the $14s11p5d$-$2s2p3s3p3d$ CAS [Fig. 1(b)]. Crosses on each trajectory throughout the paper show a stabilized point. All trajectories show resonance points clearly along with an increased density of points. In all trajectories in this paper θ starts at $\theta = 0.01$ rad at the top and increases with a step of 0.01 rad.

Theoretical calculations for the low-lying B^- $1s^22s^22p^2\ {}^1D$ shape resonance have been carried out by Johnson and Rohrlich [46], Schaefer *et al.* [47], Hunt and Moiseiwitsch [48], Moser and Nesbet [49,50], and Sinanis *et al.* [51]. Among these only Hunt and Moiseiwitsch [48] and Sinanis *et al.* [51] gave values for both an energy position and a width. Hunt and Moiseiwitsch [48] obtained the B^- $1s^22s^22p^2\ {}^1D$ shape resonance parameters by solving the Schrödinger equation with an empirically adjusted model potential under the scattering boundary condition. An experimental measurement for these resonance parameters was given by Lee *et al.* [28]. Sinanis *et al.* [51] computed this resonance parameter systematically in the framework of the state-specific configuration interaction in the continuum and obtained a theoretical value quite consistent with this measurement [28].

In Table II we have listed theoretical results obtained by others [46–51] and experimental measurement [28]. Our best current result (the $14s11p5d$-$2s2p3s3p3d$ CAS) is consistent with both the theoretical value obtained by Sinanis *et al.* [51] and the experimental measurement by Lee *et al.* [28].

B. The $1s^22s2p^3\ {}^3D$ shape resonance

We performed calculations for the B^- $1s^22s2p^3\ {}^3D$ shape resonance. In Table III we show a summary of our results for the B^- $1s^22s2p^3\ {}^3D$ shape resonance. The obtained values for the resonance positions and width are consistent with each other. In Fig. 2 we present the θ trajectories for

TABLE V. Same as in Table I, but for the B^- $1s2s^22p^3\ {}^3D$ shape resonance.

Method	Basis set CAS	α	θ_{opt} (rad)	E_r (eV)	Γ_r (eV)
M_1	$14s11p$-$1s2s2p3s$	1	0.31	188.77	0.053
M_1	$14s11p$-$1s2s2p3s3p$	0.9	0.27	188.76	0.041
M_1	$14s11p5d$-$1s2s2p3d$	0.9	0.28	188.71	0.036
CMCSTEP	$14s11p$-$1s2s2p3s$	1	0.31	188.77	0.054
CMCSTEP	$14s11p$-$1s2s2p3s3p$	0.9	0.28	188.74	0.041
CMCSTEP	$14s11p5d$-$1s2s2p3d$	0.9	0.27	188.71	0.035

TABLE VI. Same as in Table I, but for the B^- $1s2s^22p^3\ {}^3S$ shape resonance.

Method	Basis set CAS	α	θ_{opt} (rad)	E_r (eV)	Γ_r (eV)
M_1	$14s11p$-$1s2s2p3s$	1	0.24	188.70	0.077
M_1	$14s11p$-$1s2s2p3s3p$	0.9	0.23	188.81	0.074
M_1	$14s11p5d$-$1s2s2p3d$	0.9	0.23	188.85	0.073
CMCSTEP	$14s11p$-$1s2s2p3s$	1	0.28	188.71	0.142
CMCSTEP	$14s11p$-$1s2s2p3s3p$	0.9	0.28	188.83	0.141
CMCSTEP	$14s11p5d$-$1s2s2p3d$	0.9	0.26	188.87	0.142

TABLE VII. Same as in Table I, but for the B^- $1s2s^22p^3\ {}^3P$ shape resonance.

Method	Basis set CAS	α	θ_{opt} (rad)	E_r (eV)	Γ_r (eV)
M_1	$14s11p$-$1s2s2p3s$	1	0.28	188.70	0.124
M_1	$14s11p$-$1s2s2p3s3p$	1	0.28	188.85	0.125
M_1	$14s11p5d$-$1s2s2p3d$	1	0.27	188.93	0.123
CMCSTEP	$14s11p$-$1s2s2p3s$	1	0.28	188.70	0.124
CMCSTEP	$14s11p$-$1s2s2p3s3p$	1	0.28	188.85	0.125
CMCSTEP	$14s11p5d$-$1s2s2p3d$	1	0.27	188.94	0.123

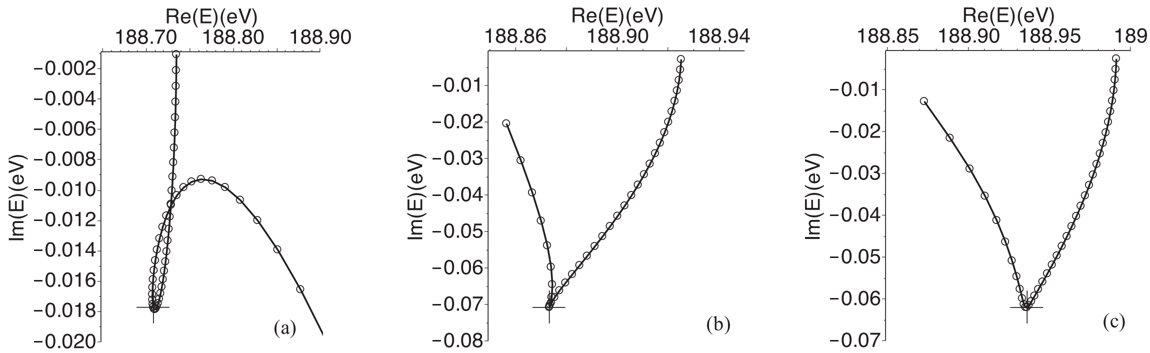

FIG. 3. The θ trajectories for B$^-$ $1s2s^22p^3\,{}^3D$ (a), ^3S (b) and ^3P (c) shape resonances obtained from the CMCSTEP method. (a)–(c) The curves correspond to the basis set $14s11p5d$ with the $1s2s2p3d$ CAS and the cross shows a stabilized point. The computational parameters are $\Delta\theta = 0.01$ rad and (a) and (b) $\alpha = 0.9$ and (c) $\alpha = 1$.

the B$^-$ $1s^22s2p^3\,{}^3D$ shape resonance obtained from the CMCSTEP method with the basis set $14s11p$-$1s2s2p3s3p$ CAS [Fig. 2(a)] and the $14s11p5d$-$2s2p3s3p3d$ CAS [Fig. 2(b)].

A theoretical prediction of the photodetachment cross section for the B$^-$ $1s^22s2p^3\,{}^3D$ shape resonance was made Ramsbottom and Bell [52]. They employed a multichannel theory based on the R-matrix method for electron-atom collisions. Moreover, other calculations [53] were based on the many-body method in the framework of the spin-polarized random-phase approximation with exchange and thereby were analogous to the calculations of the C$^-$, Si$^-$, and Ge$^-$ ions [54,55], which predicted a window-type resonance just below the B ($2s2p^2\,{}^4P$) state [56]. Later Kashenock and Ivanov [57] investigated the collective effects in B$^-$ photodetachment using many-body theory taking interchannel interactions, dynamic-core polarization, and screening effects into account. Kristensen *et al.* [29] performed the experimental measurements for the photodetachment cross section of the B$^-$ ion at photon energies ranging from 3.37 to 4.83 eV. The position and width for the B$^-$ $1s^22s2p^3\,{}^3D$ shape resonance [29] are determined by fitting the experimental photoabsorption curve to the modified Wigner threshold law [58]. Table IV shows a comparison of our results with the previously obtained values [52,57] and the extracted result from the experimental data [29]. Each value is consistent with each other.

Furthermore, the behavior of the photodetachment cross section above the threshold indicates theoretically the presence of the B$^-$ $1s^22s2p^3\,{}^3P$ shape resonance [29]. After carrying out the CMCSTEP calculation for B$^-$ $1s^22s2p^3$ (^3S,^3P) states with a basis set $14s11p5d$-$1s2s2p3d$ CAS, we obtain the following values of positions and widths for these states: $E_r =$ 4.89 (^3S) and 10.96 eV (^3P) and $\Gamma = 1.98$ (^3S) and 1.20 eV (^3P), respectively.

C. The $1s2s^22p^3\,{}^3D$, ^3S, and ^3P resonances

We have also performed the M$_1$ and CMCSTEP calculations for the B$^-$ $1s2s^22p^3\,{}^3D$, ^3S, and ^3P shape resonances. We use the $1s2s^22p^2\,{}^4P$ CMCSCF state as the initial state. In Tables V–VII we show the summaries of theoretical calculations for the B$^-$ $1s2s^22p^3\,{}^3D$, ^3S, and ^3P shape resonances, respectively. In the first three rows of each table results from M$_1$ calculations are shown, while the last three rows show results from the CMCSTEP calculations. For the ^3D shape resonance (Table V), resonance parameters from both methods are consistent with each other for the chosen basis sets. For the ^3S shape resonance (Table VI), the obtained resonance positions from the M$_1$ and CMCSTEP calculations are almost identical, however, for widths the CMCSTEP calculations give results almost two times more than those obtained by the M$_1$ calculations. All values for the ^3P shape resonance shown in Table VII are consistent with each other as well.

In Fig. 3 we show the θ trajectories for the B$^-$ $1s2s^22p^3\,{}^3D$ [Fig. 3(a)], ^3S [Fig. 3(b)], and ^3P [Fig. 3(c)] shape resonances obtained from the CMCSTEP calculations with the basis set $14s11p5d$ with the $1s2s2p3d$ CAS. Berrah *et al.* [31] presented theoretical and experimental values of resonance parameters for these ^3D, ^3S, and ^3P states. Theoretically they used two separate R-matrix methods. Moreover, they revealed three near-threshold ($E^{th} = 188.63$ eV) shape resonances that are each described by Breit-Wigner-Lorentzian profiles from experimental measurements of B$^-$ K-shell photodetachment.

TABLE VIII. Same as in Table II, but for the B$^-$ $1s2s^22p^3$ shape resonance.

Reference	E_r (eV) (^3D)	Γ_r (eV) (^3D)	E_r (eV) (^3S)	Γ_r (eV) (^3S)	E_r (eV) (^3P)	Γ_r (eV) (^3P)
[31]	188.73	0.056	189.03	0.178	189.22	0.536
this work						
M$_1$	188.71	0.036	188.85	0.073	188.93	0.123
CMCSTEP	188.71	0.035	188.87	0.142	188.94	0.123
Expt. fit [31]	188.72 ± 0.05	0.037 ± 0.020	189.03 ± 0.05	0.071 ± 0.022	189.17 ± 0.13	$0.26\,(^{+0.26}_{-0.10})$

In Table VIII we show a comparison of our results with other theoretical results [31] and extracted data from experimental measurements [31] for the B^- $1s2s^22p^3\,{}^3D$, ${}^3S$, and ${}^3P$ shape resonances. In rows 2 and 6 we place the theoretical results and experimentally fitted data for these three states obtained in Ref. [31]. The comparison demonstrates that our results for positions for ${}^3S$ and ${}^3P$ states are very slightly smaller that those in Ref. [31], however, they are consistent with that in Ref. [31] for the ${}^3D$ state. Results for widths are also smaller than that calculated by others in Ref. [31], however, our results are very close to experimentally fitted data.

IV. SUMMARY AND CONCLUSIONS

In this work we have further developed the CMCSTEP method and presented theoretical calculations for B^- shape resonances using two different but related methods (M_1 and CMCSTEP). Two different basis sets $14s11p$ and $14s11p5d$ with six different CASs are used in the calculations. In CMCSTEP calculations we use open-shell CMCSCF states as the initial states. The low-lying B^- $1s^22s^22p^2\,{}^1D$, higher B^- $1s^22s2p^3\,{}^3D$, and B^- $1s2s^22p^3\,{}^3D$, ${}^3S$, and ${}^3P$ shape resonance parameters were calculated theoretically using the M_1 and CMCSTEP methods. The M_1 and CMCSTEP values of the B^- shape resonances were compared with previously obtained calculational results and experimental measurements in the literature. The results from M_1 and CMCSTEP calculations are reliable and practical for resonance problems including for the initial- and final-state open-shell cases.

Although we have here presented results for resonance parameters for an atomic system B^-, these methods can be implemented for investigating shape resonance parameters for molecular systems as well. We had previously shown that the ${}^2\Pi_g$ $N_2{}^-$ shape resonance using the M_1 method [13] is quite consistent with previous literature results [59–62] and experimental measurements [63,64]. The N_2 initial (ground) state is totally symmetric in spin and space and has no nondynamical correlation. In the molecular case [13], the CS technique for the electron-nuclear Coulomb interaction potential $-Z/|\mathbf{r}-\mathbf{R}|$ has been implemented so that $-(Z\eta^{-1})/|\mathbf{r}-\mathbf{R}\eta^{-1}|$, where Z is a nuclear charge and $\mathbf{r}$ and $\mathbf{R}$ are the electronic and nuclear positions relative to an origin of a fixed molecular coordinate system [43]. Moreover, the CS can be modified by using basis functions with complex orbital exponents [65,66] or by using exterior complex scaling [67].

The application of the CMCSTEP method to resonance problems (shape, Feshbach, and Auger) for other open-shell and closed-shell initial-state atomic and molecular systems, including cases with nondynamical correlation in the initial state, is left for future research.

ACKNOWLEDGMENTS

We thank the Robert A. Welch Foundation for financial support through Grant No. A-770. Fruitful discussions with Dr. Songbin Zhang and Dr. K. Samanta on implementing the complex version of the codes are gratefully acknowledged.

[1] J. N. Bradsley and M. A. Biondi, Adv. At. Mol. Phys. **6**, 1 (1970).
[2] H. Massey, *Negative Ions*, 3rd ed. (Cambridge University Press, Cambridge, 1970).
[3] R. Barrios, P. Skurski, and J. Simons, J. Phys. Chem. B **106**, 7991 (2002).
[4] J. Simons, Acc. Chem. Res. **39**, 772 (2006).
[5] J. Aguilar and J. M. Combes, Commun. Math. Phys. **22**, 269 (1971).
[6] E. Balslev and J. M. Combes, Commun. Math. Phys. **22**, 280 (1971).
[7] B. Simon, Commun. Math. Phys. **27**, 1 (1972).
[8] U. V. Riss and H.-D. Meyer, J. Phys. B **26**, 4503 (1993).
[9] R. Santra and L. Cederbaum, Phys. Rep. **368**, 1 (2002).
[10] N. Moiseyev, Phys. Rep. **302**, 212 (1998).
[11] K. B. Bravaya, D. Zuev, E. Epifanovsky, and A. I. Krylov, J. Chem. Phys. **138**, 124106 (2013).
[12] K. Samanta and D. L. Yeager, J. Phys. Chem. B **112**, 16214 (2008).
[13] K. Samanta and D. L. Yeager, Adv. Chem. Phys. **150**, 103 (2012).
[14] R. Graham, D. L. Yeager, J. Olsen, P. Jørgenson, R. Harrison, S. Zarrabian, and R. Bartlett, J. Chem. Phys. **85**, 6544 (1986).
[15] K. Samanta and D. L. Yeager, Int. J. Quantum Chem. **110**, 798 (2010).
[16] J. A. Nicols, D. L. Yeager, and P. Jørgenson, J. Chem. Phys. **80**, 293 (1984).
[17] J. T. Golab and D. L. Yeager, J. Chem. Phys. **87**, 2925 (1987).
[18] R. Saha, D. Ma, and D. L. Yeager, Int. J. Quantum Chem. **107**, 694 (2007).
[19] D. Ma and D. L. Yeager, Int. J. Quantum Chem. **108**, 100 (2008).
[20] D. Ma and D. L. Yeager, Int. J. Quantum Chem. **108**, 1130 (2008).
[21] R. L. Graham, D. L. Yeager, and A. Rizzo, J. Chem. Phys. **91**, 5451 (1989).
[22] D. L. Yeager, J. A. Nichols, and J. T. Golab, J. Chem. Phys. **97**, 8441 (1992).
[23] T. Tsednee, L. Liang, and D. L. Yeager, Phys. Rev. A **91**, 022506 (2015).
[24] L. M. Branscomb and S. J. Smith, J. Chem. Phys. **25**, 598 (1956).
[25] C. S. Feigerle, R. R. Cordermann, and W. C. Lineberger, J. Chem. Phys. **74**, 1513 (1981).
[26] Y. Liu, D. J. Pegg, J. S. Thompson, J. Dellwo, and G. D. Alton, J. Phys. B **24**, L1 (1991).
[27] D. H. Lee, C. Y. Tang, J. S. Thompson, W. D. Brandon, U. Ljungblad, D. Hanstorp, D. J. Pegg, J. Dellwo, and G. D. Alton, Phys. Rev. A **51**, 4284 (1995).
[28] D. H. Lee, W. D. Brandon, D. Hanstorp, and D. J. Pegg, Phys. Rev. A **53**, R633 (1996).
[29] P. Kristensen, H. H. Andersen, P. Balling, L. D. Steele, and T. Andersen, Phys. Rev. A **52**, 2847 (1995).
[30] M. Scheer, R. C. Bilodeau, and H. K. Haugen, Phys. Rev. Lett. **80**, 2562 (1998).

[31] N. Berrah, R. C. Bilodeau, I. Dumitriu, J. D. Bozek, N. D. Gibson, C. W. Walter, G. D. Ackerman, O. Zatsarinny, and T. W. Gorczyca, Phys. Rev. A **76**, 032713 (2007).
[32] D. R. Bates, Adv. At. Mol. Opt. Phys. **27**, 1 (1991).
[33] D. Sundholm and J. Olsen, Chem. Phys. Lett. **171**, 53 (1990).
[34] C. Froese Fischer, A. Ynnerman and G. Gaigalas, Phys. Rev. A **51**, 4611 (1995).
[35] V. G. Zakrzewski, J. V. Ortiz, J. A. Nichols, D. Heryadi, D. L. Yeager, and J. T. Golab, Int. J. Quantum Chem. **60**, 29 (1996).
[36] S. Mahalakshmi and D. L. Yeager, Mol. Phys. **101**, 165 (2003).
[37] S. Mahalakshmi and D. L. Yeager, in *Fundamental World of Quantum Chemistry: A Tribute to Per-Olov Löwdin*, edited by E. J. Brandas and E. S. Kryachko (Kluwer Academic, Dordrecht, 2004), p. 547.
[38] H. Hotop and W. C. Lineberger, J. Phys. Chem. Ref. Data **14**, 731 (1985).
[39] P.-O. Löwdin, Adv. Quantum Chem. **19**, 87 (1988).
[40] S. Yabushita and C. W. McCurdy, J. Chem. Phys. **83**, 3547 (1985).
[41] D. L. Yeager and M. K. Mishra, Int. J. Quantum Chem. **104**, 871 (2005).
[42] D. J. Rowe and C. Ngo-Trong, Rev. Mod. Phys. **47**, 471 (1975).
[43] R. A. Donnelly and J. Simons, J. Chem. Phys. **73**, 2858 (1980).
[44] N. Moiseyev, S. Friedland, and P. R. Certain, J. Chem. Phys. **74**, 4739 (1981).
[45] T. H. Dunning, J. Chem. Phys. **90**, 1007 (1989).
[46] H. R. Johnson and F. Rohrlich, J. Chem. Phys. **30**, 1608 (1959).
[47] H. F. Schaefer III, R. A. Klemm, and F. E. Harris, J. Chem. Phys. **51**, 4643 (1969).
[48] J. Hunt and G. L. Moiseiwitsch, J. Phys. B **3**, 892 (1970).
[49] C. M. Moser and R. K. Nesbet, Phys. Rev. A **4**, 1336 (1971).
[50] C. M. Moser and R. K. Nesbet, Phys. Rev. A **6**, 1710 (1972).
[51] C. Sinanis, Y. Komninos, and C. A. Nicolaides, Phys. Rev. A **57**, R3158 (1998).
[52] C. A. Ramsbottom and K. L. Bell, J. Phys. B **28**, 4501 (1995).
[53] V. K. Ivanov, T. Anderson, and A. N. Ipatov, in *Europhysics Conference Abstracts*, edited by R. Vilaseca (European Physical Society, Geneva, 1994), Vol. 18D.
[54] M. Ya. Amusia, G. F. Gribakin, V. K. Ivanov, and L. V. Chernysheva, J. Phys. B **23**, 385 (1990).
[55] G. F. Bribakin, A. A. Gribakina, G. V. Gultsev, and V. K. Ivanov, J. Phys. B **25**, 1757 (1992).
[56] V. K. Ivanov and L. P. Krukovskaya, J. Phys. B **27**, 4111 (1994).
[57] G. Yu. Kashenock and V. K. Ivanov, J. Phys. B **30**, 4235 (1997).
[58] J. R. Peterson, Y. K. Bae, and D. L. Huestis, Phys. Rev. Lett. **55**, 692 (1985).
[59] T. Rescigno, A. Orel, and C. McCurdy, J. Chem. Phys. **73**, 6347 (1980).
[60] H.-D. Meyer, Phys. Rev. A **40**, 5605 (1989).
[61] S. Mahalakshmi, A. Venkatnathan, and M. K. Mishra, J. Chem. Phys. **115**, 4549 (2001).
[62] Y. Sajeev, R. Santra, and S. Pal, J. Chem. Phys. **122**, 234320 (2005).
[63] G. J. Schultz, Rev. Mod. Phys. **45**, 423 (1971).
[64] T. Sommerfeld, U. Riss, H. Meyer, L. Cederbaum, B. Engels, and H. Suter, J. Phys. B **31**, 4107 (1998).
[65] C. W. McCurdy, Jr. and T. N. Rescigno, Phys. Rev. Lett. **41**, 1364 (1978).
[66] C. W. McCurdy and T. N. Rescigno, Phys. Rev. A **21**, 1499 (1980).
[67] B. Simon, Phys. Lett. **71A**, 211 (1979).